# Mitigation of Chatter Instabilities in Milling by Active Structural Control

Jeffrey L. Dohner, James P. Lauffer, Terry D. Hinnerichs, Natarajan Shankar, Mark Regelbrugge, Chi-Man Kwan and Roger Xu, Bill Winterbauer, Keith Bridger

Approved for public release; further dissemination unlimited.

Sandia National Laboratories

# *M*itigation of Chatter Instabilities in Milling by Active Structural Control

*This work was performed by a research team led by Lockheed Martin and funded by DARPA. Team members and their organizations are given below.*

## Jeffrey L. Dohner
MEMS Device Technologies Dept.

## James P. Lauffer
Engr. Mechanics, Modeling & Simulation Dept.

## Terry D. Hinnerichs
Solid Mechanics Engineering Dept.

Sandia National Laboratories
P.O. Box 5800, Albuquerque, NM 87185-1080

## Natarajan Shankar (project lead)
Lockheed Martin Space Systems Company
3251 Hanover St., Palo Alto, CA 94304

## Mark Regelbrugge (technical lead)
Rhombus Consultants Group, Inc.
2565 Leghorn St., Mountain View, CA 94043

## Chi-Man Kwan and Roger Xu
Intelligent Automation, Inc.
7519 Standish Place, Rockville, MD 20855

## Bill Winterbauer
Ingersoll Milling Machine Company,
707 Fulton Avenue, Rockford, IL 61103

## Keith Bridger
Active Signal Technology, Inc.
13027-A Beaver Dam Road
Cockeysville, MD 21030

## Abstract

This report documents how active structural control was used to significantly enhance the metal removal rate of a milling machine. An active structural control system integrates actuators, sensors, a control law and a processor into a structure for the purpose of improving the dynamic characteristics of the structure. Sensors measure motion, and the control law, implemented in the processor, relates this motion to actuator forces. Closed-loop dynamics can be enhanced by proper control law design.

Actuators and sensors were imbedded within a milling machine for the purpose of modifying dynamics in such a way that mechanical energy, produced during cutting, was absorbed. This limited the on-set of instabilities and allowed for greater depths of cut. Up to an order of magnitude improvement in metal removal rate was achieved using this system.

Although demonstrations were very successful, the development of an industrial prototype awaits improvements in the technology. In particular, simpler system designs that assure controllability and observability and control algorithms that allow for adaptability need to be developed.

Intentionally Left Blank

# Acknowledgements

Intentionally Left Blank

# Table of Contents:

# $M$*itigation of Chatter Instabilities in Milling*

# *by Active Vibration Control*

# List of Figures:

Intentionally Left Blank

# *I*ntroduction

The following is a discussion of the design, analysis, and testing performed to demonstrate the value of using active vibration control to enhance the productive capacity of a milling machine.

Maximum Metal Removal Rate (MMRR) is a quantitative measure of the productive capacity of a machine tool. The MMRR is limited by several factors including the onset of machining instabilities that are a function of the vibratory modes of both the machine and the tool (see Merritt, 1965, Tlusty and Ismail, 1983, and Shi and Tobias, 1984).

By altering the dynamic characteristics of these modes, instabilities could be mitigated and MMRR improved. Alteration could be achieved by physically redesigning or modifying the structure of the machine; however, an alternative approach is to use an active control system to alter the system dynamics. In an active control system, actuators, sensors, computers and software replace mechanical components to provide the desired dynamic response characteristics.

Examples of the use of active systems to alter dynamics during machining are relatively few, see Comstock, Tse, and Lemon, 1969, Sadek and Tobias, 1973, Hong-Yeon Hwang, Jun-Ho Oh, and Kwang-Joon Kim, 1988, and Shiraishi, Yamanaka, and Fujita, 1990, General Dynamics Team 1998, and Redmond, Barney, and Smith, 1999. In general, most of these papers address turning, not milling.

Milling machines are designed for a set of tools with diameters similar to the diameter of the spindle. When a tool has a diameter that is much less than the diameter of the spindle, a mechanical impedance mismatch occurs between the tool and the spindle, and mechanical energy can be trapped within the tool (i.e. a tool mode). During cutting, these tool modes can become unstable. Larger diameter tools usually do not experience this phenomenon due to the power limitations of the machine. Other researchers have developed methods to avoid these instabilities by varying spindle speed (see Jemielniak and Widota, 1984,Altintas and Chan, 1992, and CRAC, 1992). However, this often requires moving to higher or lower spindle speeds where MMRR is decreased (i.e. lower spindle speeds) or where tool wear is increased (i.e. high spindle speeds).

Actively changing the dynamics of a machine can enhance MMRR without the need for changing spindle speeds. The following is a discussion of an alternate approach - the development of hardware and software constructed to enhance the MMRR of a machine tool using an active structural control system.

# *H*ardware Design

An illustration of the hardware designed and constructed to demonstrate the utility of active control is shown in Figure 1. Much of this hardware was constructed and assembled at the Ingersoll Milling Machine Company (Rockford IL).

As shown in Figure 1, vibration is sensed at the root of a rotating tool by strain gages that are arranged in half bridge configurations to sense bending in two lateral directions. Excitation voltages were supplied to the half bridges using commercial electronics. Power is supplied to these electronics via magnetic coupling between rotating and stationary wires.

A telemetry system is used to transmit strain data from the rotating spindle to stationary receivers. Both the rotating and stationary electronics were fabricated by the Wireless Data Corporation (see Wireless Data).

Strain is measured in a coordinate system that rotates with the shaft, $(x, y, z)$, however, actuation occurs in a coordinate system that is stationary with the machine, $(X, Y, Z)$. Therefore, the strain data must be translated from rotating to stationary coordinates. To do this, the angular position of the spindle is measured using a decoder. Decoder and strain-gage-bridge voltages are fed into anti-aliasing filters, analog to digital converters (A/D), and a processor for the computation of this transformation. The anti-aliasing filters, the A/Ds, and the processor are part of a component called a controller.

A controller is a hardware component with the ability to capture voltage signals, combine them in accordance with a defined mathematical relationship, and output the result as another set of voltage signals. Intelligent Automation Inc. (Rockville, MD) designed and fabricated the controller discussed in this paper.

For our application, the control law operates on stationary strain signals and feeds back activation signals to the actuators. Control laws were designed to absorb energy from the rotating tool thereby, reducing entrapped energy. This absorption of energy increases the stability of the cutting process and improves MMRR. The control law is defined by programmable logic.

As shown in Figure 1, the controller produces four voltage signals that drive a set of four power amplifiers. These power amplifiers drive stacks of electrostrictive material (PMN) embedded within the housing of the machine. These stacks (produced by Lockheed Martin Corporation and integrated into the housing by Active Signal Inc.) produce force against a non-rotating portion of the machine called the cartridge. The spindle moves with the center line of the cartridge and floats on a hydrostatic bearing. Thus, forces on the cartridge produce motions in the tool. Motions corresponding to tool bending can be sensed by the strain gages and fed back into the control system.

Hardware, consisting of the spindle, the tool holder, the cartridge, the actuators, part of the telemetry system, and much of the surrounding housing was given the special name - the Smart Spindle Unit (SSU). A photograph of the SSU is shown in Figure 2. Separate from the SSU are the power amplifiers, the controller, and the telemetry package receiver.

decoder

hydrostatic bearing

electrostrictive actuators

cartridge

ball bearings

spindle (rotating)

telemetry package and bridge electronics (rotating)

strain gages at tool root

cutting tool

cutting excitation

telemetry power supply and receiver antenna (stationary)

cross section of Smart Spindle Unit (SSU)

power amplifiers     controller     telemetry receiver

Figure 1. Hardware Configuration

11
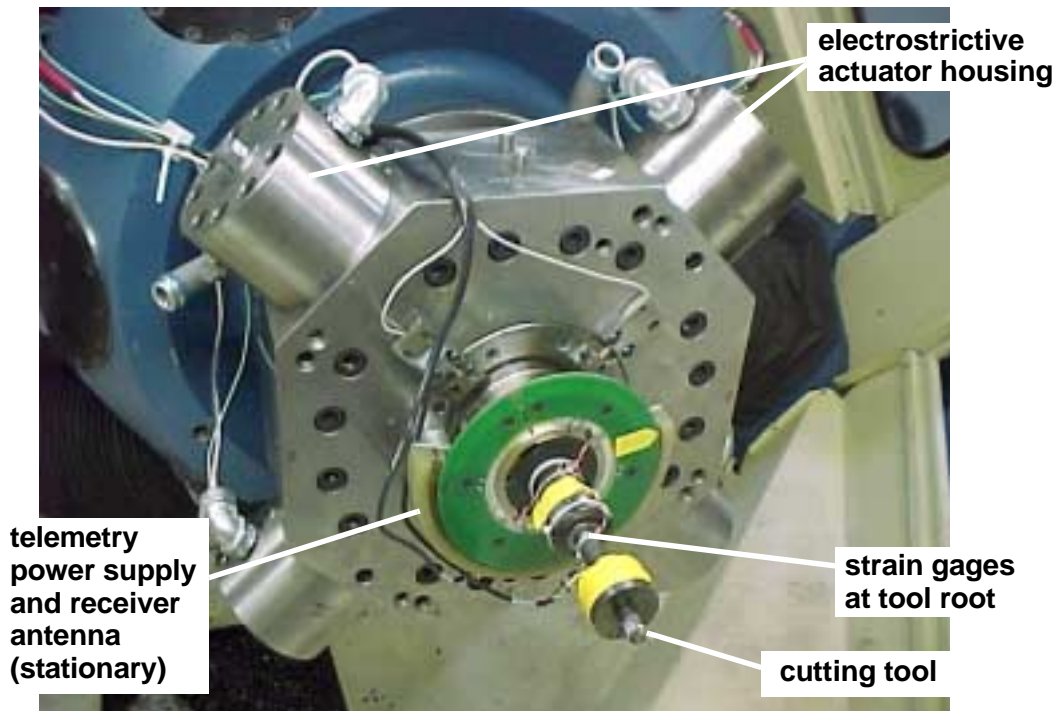
Figure 2. Modified Tool and Smart Spindle Unit

# *C*haracterization

Without the benefit of previous design data, the SSU design relied heavily on the use of numerical analysis (see Dohner et. al., 1997). Although this allowed for enough insight to complete an initial design, a full characterization of dynamics was required upon fabrication.

Initial experimental analysis of the SSU showed that system dynamics were not controllable or observable (see Kwakernaak and Sivan, 1972 for an explanation of controllability and observability). Frequency Response Functions (FRFs) were measured between voltage inputs to the power amplifiers and tool strain responses in stationary coordinates. Initial measurements were made with the spindle at rest (0 rpm). Figure 3, is a plot

of the Maximum Singular Values (MSVs) of these FRFs. The MSVs give a bound of the FRF response of the system. From the MSVs the modes of the system can be identified. The first "tool" mode occurred at about 800Hz, however, as shown in this figure, it participated little in the response. Thus, a state space model derived from the measured FRFs would not be controllable or observable.

The reason the system was neither controllable nor observable was because of an anti-resonance in the FRFs between the actuators and strain sensors. The frequency of the anti-resonance occurred at virtually the same frequency as the fundamental mode of the tool. The anti-resonance was due to modal cancellation between rigid-body modes of the cartridge/spindle system.
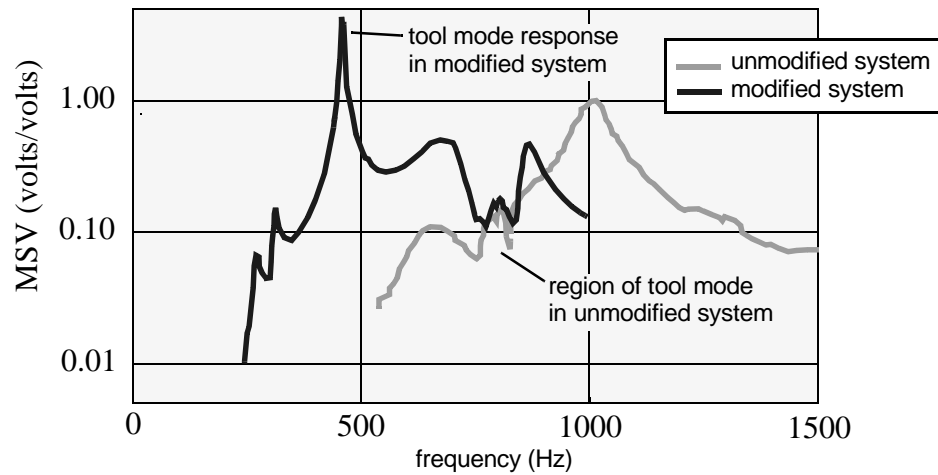
Figure 3. Maximum Singular Value of FRFs Showing the Location of the Tool Mode

Controllability and observability could have been achieved by shifting the resonant frequencies of the cartridge and spindle to frequencies above the fundamental frequency of the tool; however, to do this would have required a complete redesign of the SSU, and such modifications were beyond available budget and time.

Therefore, two options were available:

option 1) *fabricate* a longer more flexible tool with a lower fundamental frequency, or

option 2) *modify* the existing tool to lower its fundamental frequency.

Due to budget constraints, the second option was chosen. A mass was added close to the end of the existing tool to move the fundamental tool mode away from any rigid-body anti-
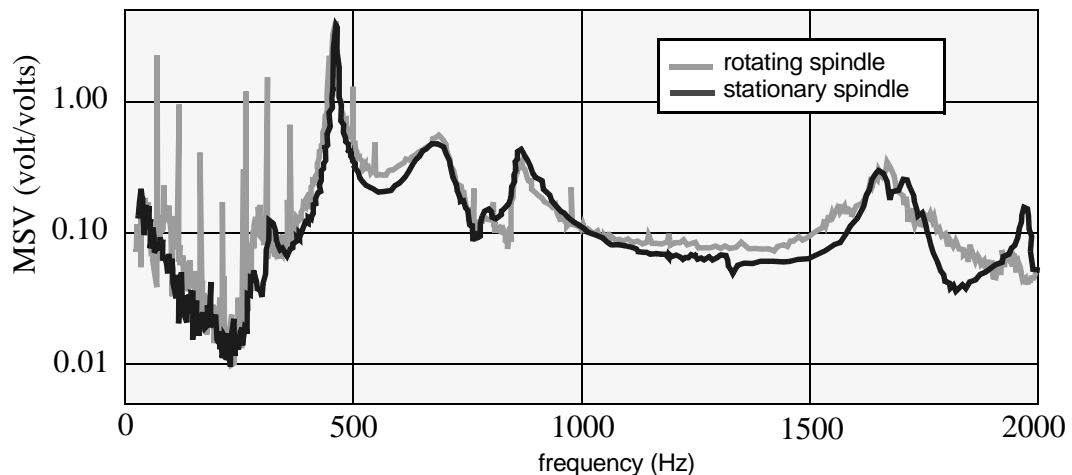


Figure 4. Maximum Singular Value of FRFs for Rotating and Stationary Spindles

13
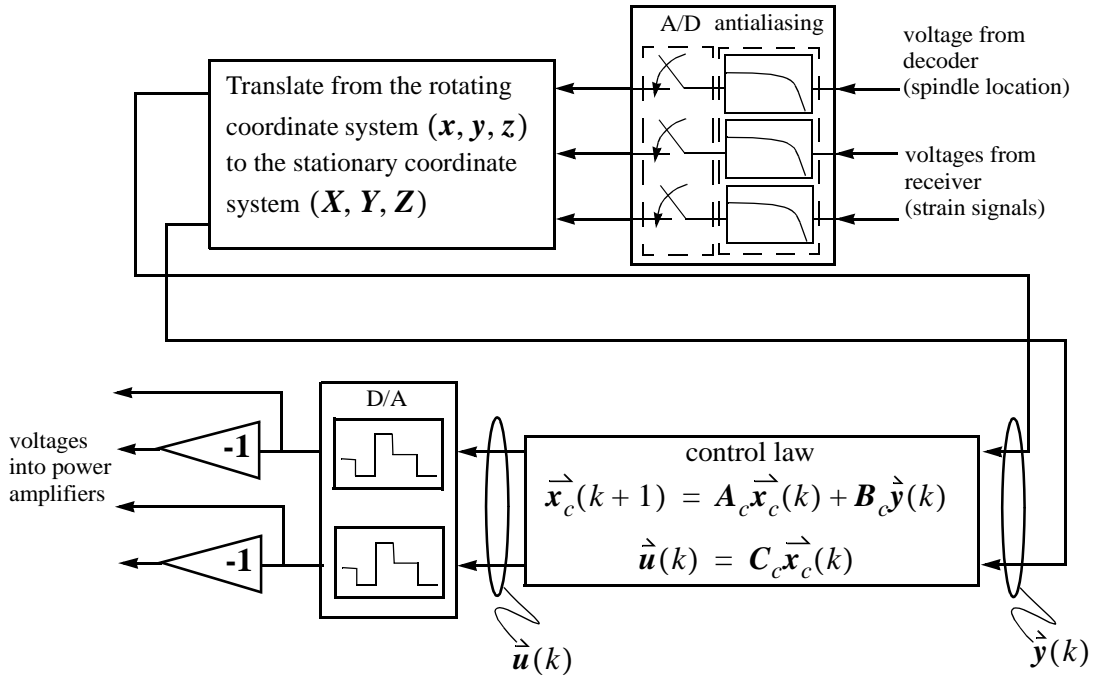
Figure 5. Controller Function in Block Diagram Form

resonance. Subsequent FRFs are shown in Figure 3. As shown, the tool mode (now clearly visible) was shifted from 800 Hz down to 453 Hz. The resulting realization (state space model) of the modified system was both controllable and observable.

Additional measurements were performed to determine how FRFs varied with rotation. In Figure 4 the maximum singular value of the actuator to strain FRFs for both rotating (3000 RPM) and stationary conditions are shown. The main difference between these plots is the presence of harmonics at multiples of the rotational speed of the spindle. These harmonics are artifacts due to bearing inputs, out-of-roundness, and balancing that could have been reduced by using more ensemble averages when estimating the FRFs.

More importantly, Figure 4 shows that the dynamics of the fundamental

mode appears to be invariant with respect to rotation speed. Therefore, the same control law can be used regardless of the spindle rotation speed.

# $C$ontrol Design

Control design was performed as a two step process.

step 1) The production of a reduced order realization of dynamics, and

step 2) The design of a robust controller.

Figure 5 shows controller logic. Three voltage signals are fed into the controller - two voltage signals from the receiver and a voltage signal from the decoder. These signals are passed through anti-aliasing filters and are

14

then sampled. The result is a numerical data train representing tool strain, in rotating coordinates, $(x, y, z)$, and spindle location. This data is combined to calculate tool strain in the stationary coordinate system $(X, Y, Z)$ (as discussed above).

At sample time $k$, stationary strain data is given in vector form by

$$\vec{y}(k) = \begin{bmatrix} \varepsilon_X(k) \\ \varepsilon_Y(k) \end{bmatrix}$$

where $\varepsilon_X(k)$ and $\varepsilon_Y(k)$ is sampled, stationary, strain data in the $X$ and $Y$ planes. This vector is used by the control law to compute the outputs of the controller. The control law takes the form

$$\vec{x}_c(k + 1) = A_c\vec{x}_c(k) + B_c\vec{y}(k) \quad (1.a)$$

$$\vec{u}(k) = C_c\vec{x}_c(k) \quad (1.b)$$

where $A_c \in \mathfrak{R}^{nxn}$ is the controller state matrix, $B_c \in \mathfrak{R}^{nx2}$ is the controller input matrix, $C_c \in \mathfrak{R}^{2xn}$ is the controller output matrix, and $n$ is the number of states in the controller (see Kwakernaak and Sivan 1972). For this application, the control law was designed to absorb energy from the system; consequently, closed-loop tool dynamics are more heavily damped than open-loop tool dynamics. The state, input and output matrices are chosen in such a way that this form of energy absorption occurs.

Using the control law and the data train, $\vec{y}(k), \vec{y}(k-1), \vec{y}(k-2)...$, the output vector,
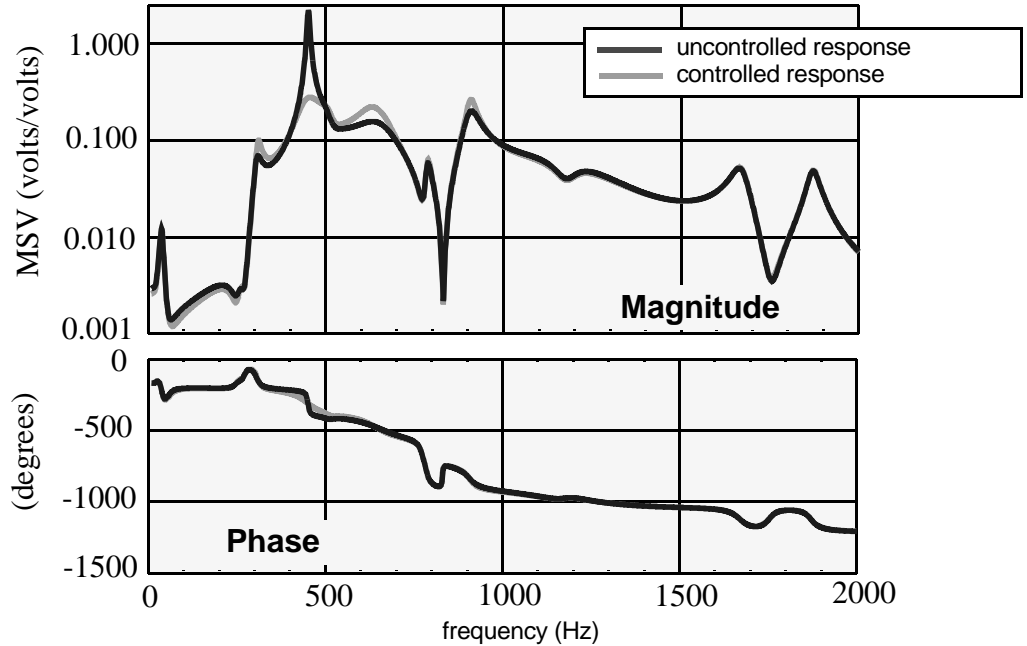


Figure 6. Frequency Response Function, Magnitude and Phase, With and Without Control

$$\vec{u}(k) = \begin{bmatrix} u_1(k) \\ u_2(k) \end{bmatrix},$$

can be calculated. The output vector data train is converted into two analog voltage signals by a set of digital to analog converters (D/A). Because of the cruciform configuration of the SSU, actuators on either side of the cartridge were assumed to move the same amount; therefore, voltage signals into the power amplifiers can be formed by splitting each D/A output voltage and changing the sign on one of the signals.

In order to choose a controller state, input, and output matrix that will damp tool motion, a mathematical realization of dynamics from $\vec{u}(k)$ to $\vec{y}(k)$ must be produced. This realization is often referred to as the plant. A variety of algorithms can be used to produce a plant realization from measured frequency response func-

tions. The algorithm used in this effort was the Eigensystem Realization Algorithm with Direct Correlations, ERA/DC, (see Juang, 1994). Neglecting any direct feed through effects, this algorithm produces a realization of the form

$$\vec{x}(k+1) = A\vec{x}(k) + B\vec{u}(k) \quad (2.a)$$

$$\vec{y}(k) = C\vec{x}(k) \quad (2.b)$$

where $A \in \mathfrak{R}^{nxn}$ is the plant state matrix, $B \in \mathfrak{R}^{nx2}$ is the plant input matrix, and $C \in \mathfrak{R}^{2xn}$ is the plant output matrix. Again, $n$ is the number of states.

The control law, equation 1a,b, is a mathematical relationship from $\vec{y}(k)$ to $\vec{u}(k)$. The plant, equation 2a,b, is a mathematical relationship from $\vec{u}(k)$ to $\vec{y}(k)$. Initially, a Linear Quadratic Gaussian (LQG) approach (see
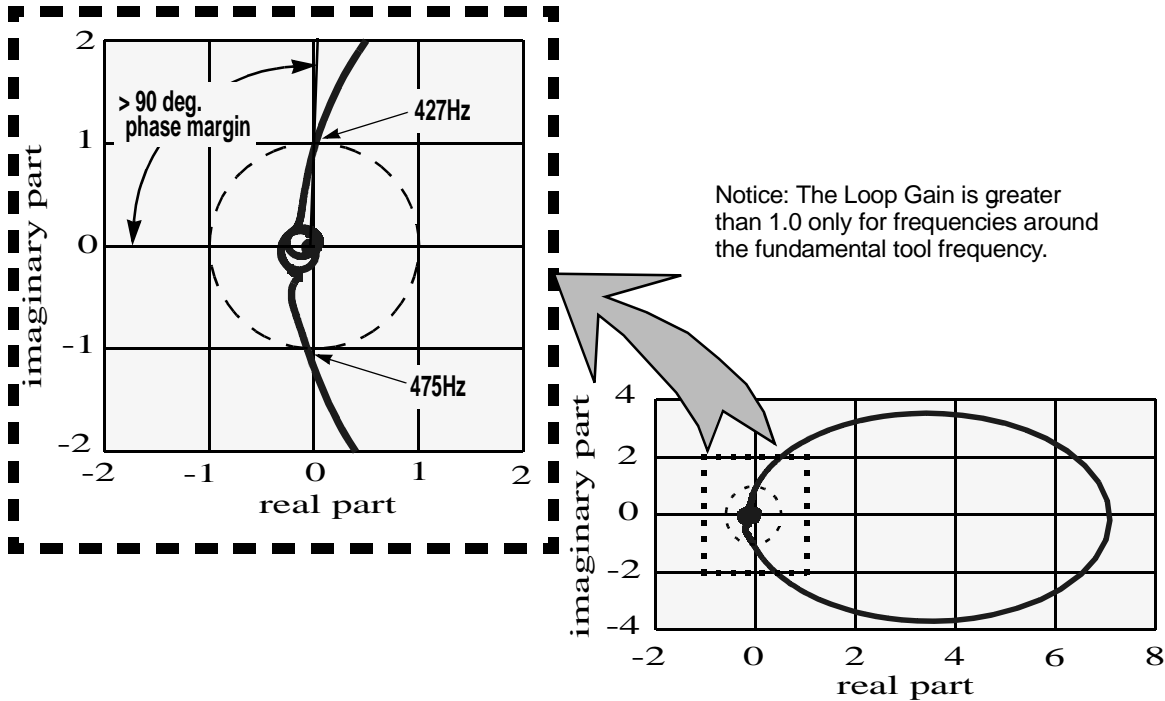


Figure 7. Nyquist Diagram of Loop Gain

16

Kawakernak and Sivan) was used to determine the state, input and output matrices of the control law. As with most uses of LQG, the weighting matrices used to define performance were manipulated to shape the loop until a sufficient balance between performance and robustness was achieved. Surprisingly, in doing this, it was found that LQG produced high levels of both robustness and performance. This occurred even for low order plant realizations $(n = 4)$.

After examination of the control law and plant, a better understanding of control dynamics was developed. Figure 6 shows a Bode plot of the plant with and without control. Notice that there is one dominant mode in this system at 450Hz. This is the tool mode. This tool mode has a peak response that is almost an order of magnitude greater than the response of any other mode in the system. Therefore, the plant can be approximated as a second order system cascaded with all pass dynamics (see Oppenheim, A.V., Schafer, R.W., 1975). Considering symmetry and neglecting cross coupling, the plant can be approximated by

$$H(s) = C(Is - A)^{-1}B = \begin{bmatrix} \Gamma(s) & 0 \\ 0 & \Gamma(s) \end{bmatrix}$$

where $\Gamma(s) = \dfrac{\phi(s)K_s}{s^2 + 2\zeta\omega_n s + \omega_n^2}$,

$|\phi(s)| = 1$ and $s$ is the Laplace transform variable.

The LQG approach produced controllers that can be approximated by

$$G(s) = C_c(Is - A_c)^{-1}B_c = \begin{bmatrix} \Theta(s) & 0 \\ 0 & \Theta(s) \end{bmatrix}$$

where $\Theta(s) = \dfrac{K_c s + \alpha}{s^2 + 2\zeta_c\omega_c s + \omega_c^2}$.

Notice that this is a Positive Real (PR) control law even through the plant was not PR. Nevertheless, because it looks unimodal in any one direction, the PR control law was adequate to produce high levels of performance with sufficient levels of robustness.

To better understand this, notice that for $\omega \approx \omega_c$ and moderate values of $K_s$ and $K_c$ the loop gain, $\Theta(s)\Gamma(s)$, is greater than 1.0 only for frequencies near to $\omega$. At all other frequencies the closed loop system is gain stabilized. This has a significant influence on the Nyquist diagram of the loop gain. Figure 7 shows the Nyquist diagram of the loop gain for a typical control law. The Nyquist diagram contains a single lobe that occurs near the fundamental frequency of the tool. The rotation and size of this lobe is controlled by the parameters $K_c$, $\zeta_c$, and $\alpha$. LQG selects these parameters such that the lobe is always deep in the right hand plane of the Nyquist diagram. This gives high loop gains and therefore good performance while also maintaining robustness (over 90 degrees of phase margin at high gain margins). Thus, for this plant, LQG was able to produce a robust, high performance, low order control law. The final control law contained only four states.

# $R$esults

Chatter instabilities occur during cutting due to dynamic feedback between
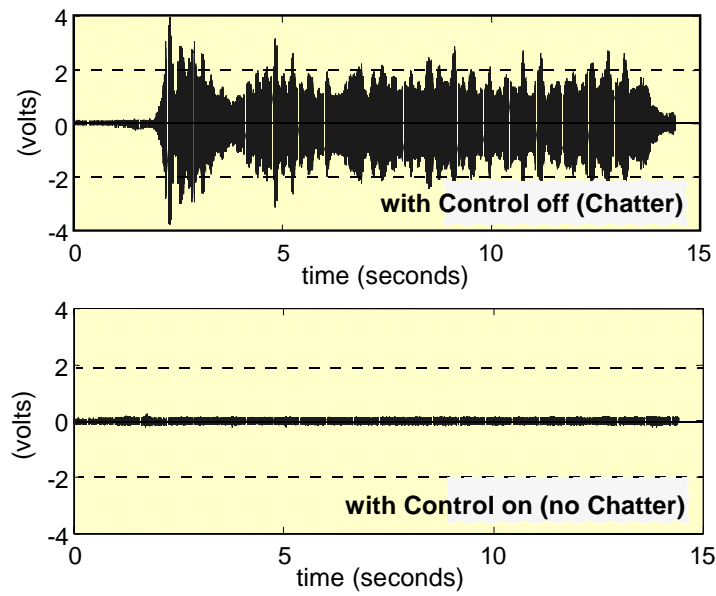
Figure 8a. Unstable and Stable Dynamic Response (time domain), Strain Response for a 0.01 mm Depth of Cut at 3600 rpm.
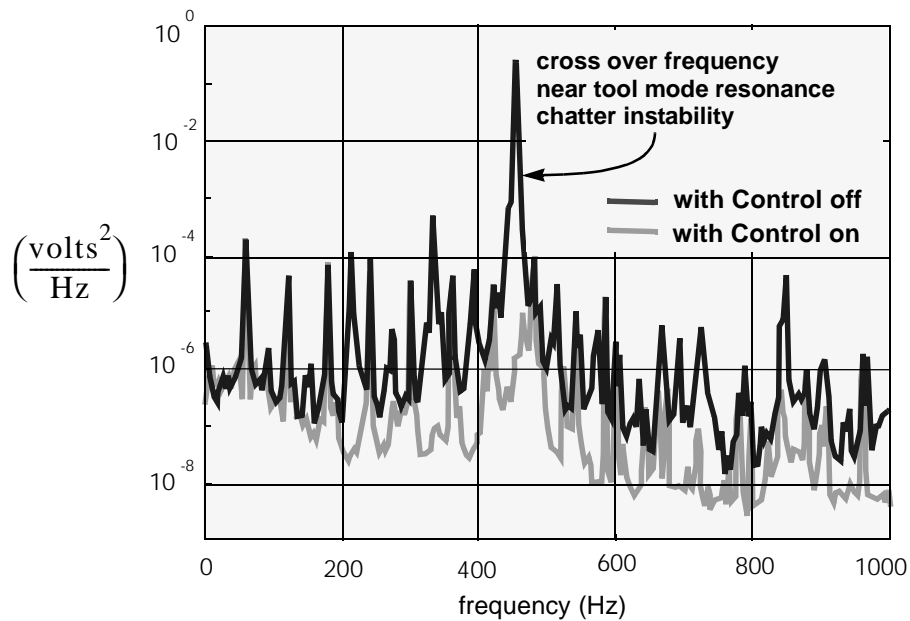


Figure 8b. Power Spectral Densities of Unstable and Stable Dynamic Responses Shown in Figure 8a
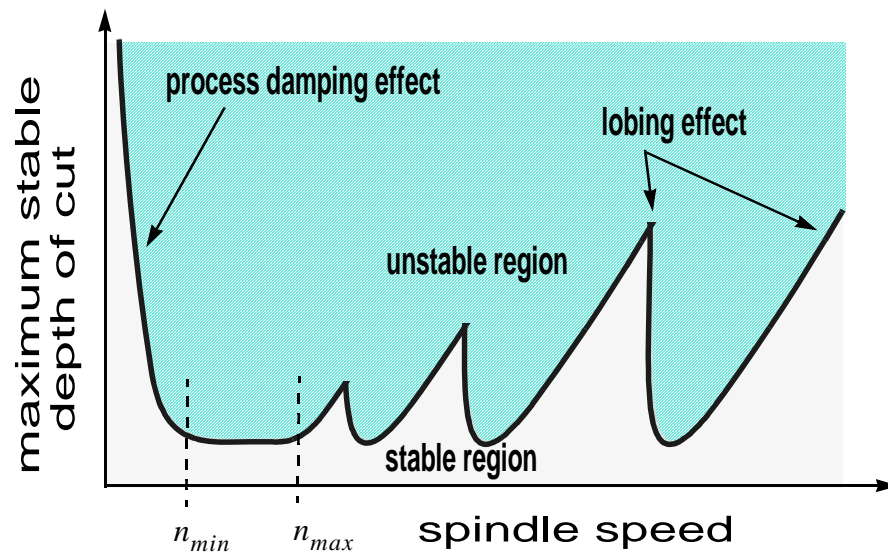
Figure 9. Stability Limits of a Typical Machine Tool

tool inserts. A cutting tool can have a number of inserts. As an insert cuts through metal it lays down a pattern, and this pattern affects the cut of the next insert on the tool. This interaction creates a dynamic feedback path between successive cuts, and, as in many feedback systems, can lead to instability. During cutting, energy is pumped into well coupled modes. If the pattern on the part is great enough that energy gain is not balanced by energy loss, energy storage will grow; thereby, producing the dynamic instability known as regenerative chatter.

Cutting instabilities can pump enough vibrational energy into the tool to eject the insert from the part. At ejection, the forces on the tool are relieved and the insert bounces back into the metal. This ejection and reimmersion creates a non-linear dynamic limit cycle process that results in severe vibration in the machine and poor surface finish.

Figure 8a,b show the response of the strain gages for a tool in chatter and a tool not in chatter. Notice that chatter can produce over an order of magnitude change in the dynamic response of the tool for a 0.01 mm depth of cut at 3600 rpm spindle speed.

Figure 9 is a cartoon of the stability limits of a hypothetical machine and tool. The area below the curve is stable and the area above the curve is unstable (unstable is hatched). Notice, that at low spindle speeds, large depths of cut can be taken; however, metal removal rate, MRR, is low due to low rotational speeds. At higher rotational speed, lobing exists. This lobing represents regions of stability. Operating within these lobes will produce high MRRs; however, for many poorly thermally conducting materials, this will also result in high tool wear caused by elevated temperatures. Therefore, most machine tools operate at intermediate spindle speeds between spindle speeds
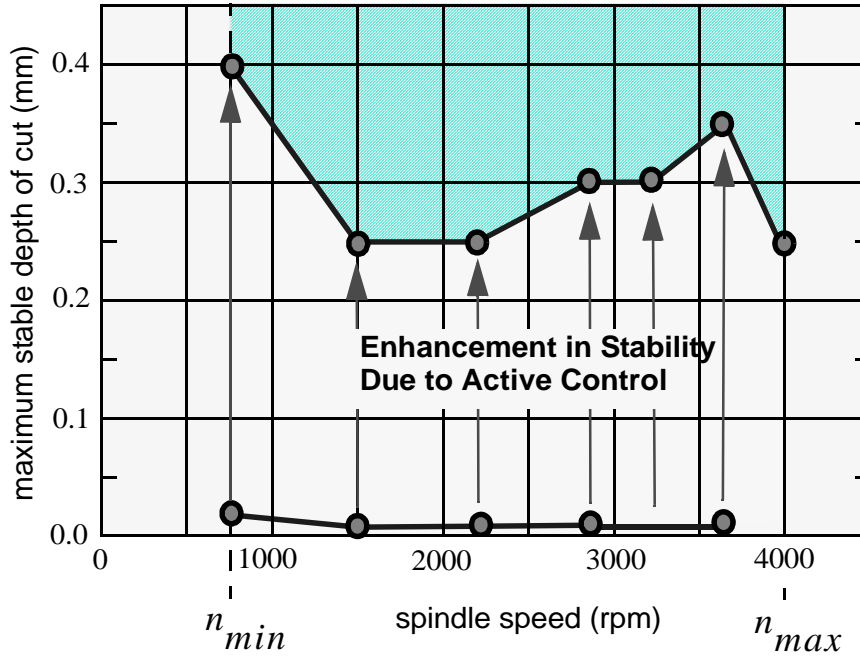
Figure 10. Enhancement in Stability Due to Active Control

$n_{min}$ and $n_{max}$. For the machine discussed in this paper, $n_{min} \approx 700 rpm$ and $n_{max} \approx 4000 rpm$.

The stability limits of the machine shown in Figure 2 were determined for control on and control off. Per ANSI/ASME standards, chip loading for full immersion cutting was held to 0.1mm/insert. Figure 10 shows the change in machine stability due to control. As shown, an *order of magnitude* increase in the maximum stable depth of cut occurred. Active vibration control significantly increased the cutting performance of this machine tool.

Other cutting tests (quarter and half immersion tests) demonstrated improved MMRR with lower levels of performance. For these tests, the maximum stable depth of cut increased by factors of 4 to 5.

# $C$onclusions

This project demonstrated that active structural control can be used to increase the MMRR of a milling machine by more than an order of magnitude. Although these results are very promising, there are still practical limitations to this technology. In particular, better methods of design, and control are required.

The design of machines that can properly leverage the use of active control is an evolving area of study. These machines must be designed to allow for the full observability and controllability of the vibration modes of interest. For this effort, the tool was altered to overcome this problem, however, in a

more mature system, this type of alteration would not be acceptable.

Because actuation and sensing occurred in two separate coordinate systems, one rotating and the other stationary, the control system was needlessly complex. This complex control system, necessary in a proof of concept experiment could be significantly simplified in a production system; such as its packaging in a compact tool holder configuration (see General Dynamics, 1998).

Active control changes the dynamics of the machine such that chatter instabilities occur at much higher depths of cut. At present, this requires the intervention of an operator. However, theoretically, the machine could be given sufficient intelligence to make these changes on its own.

# $R$eferences

Altintas, T. and Chan, P.K., 1992, "In Process Detection and Suppression of Chatter in Milling", *International Journal of Machine Tools Manufacturing*, vol. 32, no. 3, pp329-347.

Comstock, T.R., Tse, F.S., Lemon, J.R., 1969, "Application of Controlled Mechanical Impedance for Reducing Machine Tool Vibrations", *Journal of Engineering for Industry, Transactions of the ASME*, pp. 1057-1062.

*CRAC, Chatter Recognition and Control System*, 1992, MLI Manufacturing Laboratories, Inc. Gainesville, Florida, U.S. Patent No. 5,170,358.

Dohner, J.L., Hinnerichs, T.D., Lauffer, J.P., Kwan, C.M., Regelbrugge, M.E., and Shankar, N., 1997, *Proceedings of SPIE, Smart Structures and Materials, Industrial and Commercial Applications of Smart Structures Technologies*, March.

General Dynamics, Advanced Technology Systems, Guilford Center, 1998 "Precision Machining - Active Structural Control Milling Concept Demonstration System", Air Force Research Laboratory Report, AFRL-ML-WP-TR-1998-4118, June.

Hong-Yeon Hwang, Jun-Ho Oh, and Kwang-Joon Kim, 1988, "Modeling and Adaptive Pole Assignment Control in Turning", *International Journal of Machine Tool Design Research*, vol. 29, no. 2, pp. 275-285.

Jemielniak, K., and Widota, A., 1984, "Suppression of Self-Excited Vibration by the Spindle Speed Variation Method", *International Journal of Machine Tool Design Res.*, vol. 24, no. 3, pp 207-214,

Juang, Jer-Nan,. 1994, *Applied System Identification*, Englewood Cliffs, N.J., Prentice Hall.

Kwakernaak, H., and Sivan, R., 1972, *Linear Optimal Control Systems*, Wiley-Interscience, New York, N.Y.

Merritt, H.E., 1965, "Theory of Self-Excited Machine-Tool Chatter, Con-

tribution to Machine-Tool Chatter, Research--1", *Journal for Engineering for Industry, Transactions for the ASME*, pp. 447-453, November.

Oppenheim, A.V., Schafer, R.W., 1975, *Digital Signal Processing*, Prentice-Hall, Inc. Englewood Cliffs, NF.

Redmond, J., Barney, P., and Smith, D., 1999 "A Biaxial Actively Damped Boring Bar for Chatter Mitigation", *The International Journal for Manufacturing Science and Production,* Vol. 2, No. 1, pp. 1-16.

Sadek, M.M., Tobias, S.A., 1973, "Reduction of Machine Tool Vibration", *American Society of Mechanical Engineering, Applied Mechanics Division,* v1, for Meeting, Cincinnati, Ohio, pp. 128-172, September.

Shi, H.M. and Tobias, S.A., 1984, "Theory of Finite Amplitude Machine Tool Instability", *International Journal of Machine Tool Design Research*, vol. 24, No.1. pp. 45-69.

Shiraishi, M., Yamanaka, K., and Fujita, H., 1991 "Optimal Control of Chatter in Turning", *International. Journal of Machine Tools in Manufacturing*, vol. 31, No. 1, pp.31-43.

Tlusty, J., and Ismail, F., 1983, "Special Aspects of Chatter in Milling", *Journal of Vibration, Acoustics, Stress, and Reliability in Design, Transactions of ASME*, vol. 105, pp. 24-32, January.

Wireless Data Corporation, 620 Clyde Avenue, Mountain View, CA 94043

# Distribution List

MS9405 8700 R. H. Stulen
MS9402 8724 K. Wilson
MS9403 8723 J. Wang
MS9161 8726 Er-Ping Chen
MS9042 8727 J. L. Handrock
MS9042 8727 J.P. Lauffer (10)

MS1080 1749 J.F. Jakubczak II
MS1080 1749 J. J. Allen
MS1080 1749 J.L. Dohner (10)

MS0892 1715 S.J. Martin

MS0847 9120 H.S. Morgan
MS0847 9124 D.R. Martinez
MS0847 9124 J.M. Redmond
MS0847 9124 D.J. Segalman
MS0847 9124 C.R. Dohrmann
MS0847 9124 R.V. Field
MS0847 9124 D.W. Lobitz
MS0847 9126 R. May
MS0847 9126 T.D. Hinnerichs (5)

MS0835 9140 J. M. McGlaun
MS0828 9100 T.C. Bickel
MS0824 9130 J. L. Moya
MS0824 9110 A. C. Ratzel

MS0557 9125 T.J. Baca
MS0501 2338 Ming Lau
MS0501 2338 P.S. Barney

Natarajan Shankar
Lockheed Martin Space Systems Company
3251 Hanover St.
Palo Alto, CA 94304

Mark Regelbrugge
Rhombus Consultants Group, Inc.
2565 Leghorn St.
Mountain View, CA 94043

Chi-Man Kwan and Roger Xu
Intelligent Automation, Inc.
2 Research Place, Suite 202
Rockville, MD 20850

Bill Winterbauer
Ingersoll Milling Machine Company
707 Fulton Avenue
Rockford, IL 61103

Keith Bridger
Active Signal Technology, Inc.
13027-A Beaver Dam Road
Cockeysville, MD 21030

Dr. Jer-Nan Juang
NASA Langley Research Center
Mail Stop: 297
Hampton, VA 23665-5225

Richard Pappa
NASA Langley Research Center
Mail Stop: 230
Hampton, VA 23665-5225

Dr. Roy R. Craig
University of Texas at Austin
ASE-EM Department
Austin, TX 78712-1085

Dr. Robert E. Skelton
Prof. of Aeronautical & Astronautical Engineering
323 Grissom Hall
West Lafayette, IN 47907

MS9018 8945-1 Central Tech. Files
MS0899 9616 Tech. Library (2)
MS0612 9612 Review & Approval
Desk (1) For DOE/OST I

Intentionally Left Blank

# - NOTES -